

Balloon 090100001: A bright, high amplitude sdB pulsator[★]

R. Oreiro^{1,2}, A. Ulla², F. Pérez Hernández^{1,3}, R. Østensen⁴, C. Rodríguez López², and J. MacDonald⁵

¹ Instituto de Astrofísica de Canarias, 38200, Spain

² Departamento Física Aplicada, Universidade de Vigo, 36200, Spain
e-mail: ulla@uvigo.es; cristinatrl@uvigo.es

³ Departamento Astrofísica, Universidad de La Laguna, 38200, Spain
e-mail: fph@ll.iac.es

⁴ Isaac Newton Group of Telescopes, 37800 Santa Cruz de La Palma, Spain
e-mail: roy@ing.iac.es

⁵ Department of Physics and Astronomy, University of Delaware, Newark, DE1976, USA
e-mail: jimmacd@udel.edu

Received 18 November 2003 / Accepted 8 January 2004

Abstract. We report the discovery of pulsations in the light curve of Balloon 090100001, a bright sdB star ($B = 11.8$) from the balloon-borne survey of Bixler et al. (1991). Our time series observations made with the IAC80 telescope reveal a powerful short period oscillation with a period of 356 s and an amplitude (~ 59 mmag) only matched in all of the sdB pulsators by the main pulsation of PG 1605+072. The first harmonic (at 178 s) and another independent period (at 264 s) are also present in the amplitude spectrum of this new EC 14026 star. New spectroscopic data from the William Herschel Telescope provide the parameters $T_{\text{eff}} = 29\,446 \pm 500$ K and $\log g = 5.33 \pm 0.10$ dex. These place Balloon 090100001 in the low temperature and low gravity corner of the sdBV instability region, making it an interesting target for study of possible frequency changes due to stellar evolution.

Key words. stars: early-type – stars: subdwarfs – stars: oscillations – stars: individual: Balloon 090100001

1. Introduction

Disentangling the properties of the hot subdwarf phase is very important, as this stellar state corresponds to one of the last evolutionary stages of a low mass star. Although their evolutionary path is not yet well understood, hot subdwarfs are thought to be descendents of red giant stars that have undergone substantial mass loss, so much that they bypass the asymptotic giant branch and evolve directly into white dwarfs. The sdB stars are hot subdwarfs, with a canonical mass of $0.5 M_{\odot}$, that are burning He in their cores. Their location in the HR diagram, with T_{eff} between 20 000–40 000 K and $\log g$ in the range 5.25–6.50 dex, corresponds to the Extended Horizontal Branch (EHB) region (Saffer et al. 1994; Dorman et al. 1993). The EHB is defined as the blue extension of the Horizontal Branch, in which stars have a ratio $M_{\text{core}}/M_{\text{star}} \approx 0.95$ and a tiny H envelope ($\leq 0.02 M_{\odot}$). The EHB stars behave almost like He Main Sequence stars (Heber 1986).

The discovery of pulsations in some of the hot subdwarf type-B objects (sdBs) allows us to improve our knowledge of the nature of these stars by making use of asteroseismological techniques. The first pulsating sdB, EC14026-2647, discovered in 1997 (Kilkenny et al. 1997), is the prototype of a new class of pulsating objects. EC14026 stars have T_{eff} and $\log g$ in the ranges 28 400–35 700 K and 5.25–6.11 dex respectively. Their pulsation frequencies, in the range 1.8–12 mHz (80–560 s), theoretically correspond to p modes of low radial order (Charpinet et al. 1997). Currently 32 EC14026 stars are known and, although the dispersion in the observed period window is understood in terms of the frequency dependence on the physical parameters (Charpinet et al. 2002a), there exist some differences in the pulsation amplitudes too.

We report the discovery of a new pulsating sdB with an amplitude of the dominant mode similar to that of PG 1605+072 (Koen et al. 1998), but with a less populated amplitude spectrum (at least at our resolution). Balloon 090100001 ($\alpha_{2000} = 23^{\text{h}}15^{\text{m}}21^{\text{s}}.3$, $\delta_{2000} = 29^{\circ}05'01''$) was identified in a survey using a wide field-of-view balloon-borne telescope to detect FUV-bright objects (Bixler et al. 1991, hereafter BBL91). From their spectroscopic follow-up BBL91 derived $T_{\text{eff}} = 32\,500 \pm 6700$ K, $\log g = 6.00 \pm 0.69$ dex and $N(\text{He})/N(\text{H}) < 0.010$, values that place this object in the middle

Send offprint requests to: R. Oreiro, e-mail: ror@ll.iac.es

[★] Based on observations made with the IAC80 telescope operated in the Spanish Observatorio del Teide (Tenerife) and in the William Herschel Telescope (WHT) operated in the Spanish Observatorio del Roque de Los Muchachos (La Palma island).

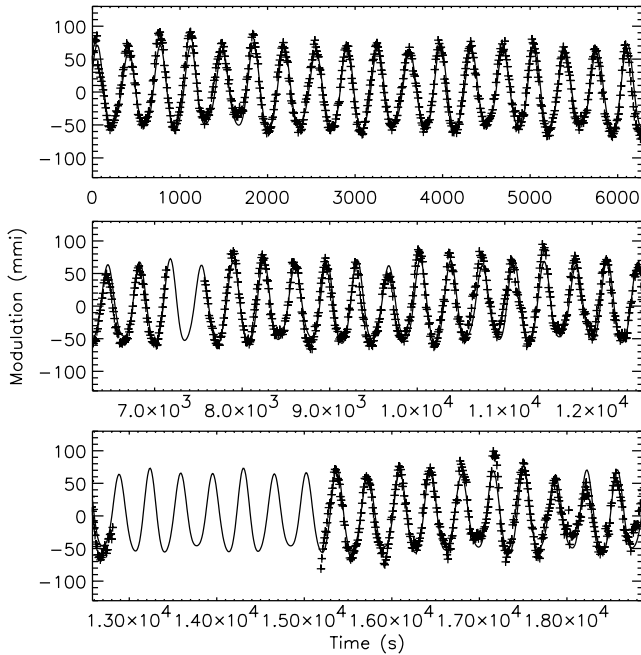


Fig. 1. Light curve of Balloon 090100001. Time starts at 23h43m10 UT on September 4, 2003 and is given in seconds. The signal is expressed in units of milli-modulation intensity (mma). Data are represented with plus-symbols and the sinusoidal fit with a continuous line. Two gaps due to instrumental problems can be seen. See text for details.

of the sdB instability region. According to our observations, Balloon 090100001 shows a large oscillation amplitude (~ 59 mma) at 2.81 mHz and at least one other mode of pulsation with a frequency of 3.78 mHz.

2. Observations

2.1. Fast photometric observations

We selected Balloon 090100001 (hereafter BA09) from a list containing temperatures and gravities of more than 600 subdwarf stars collected from the literature. Our selection was based on the target's location in the $(T_{\text{eff}}, \log g)$ plane, its brightness and its favourable coordinates for our observational campaign undertaken from August 29 to September 4, 2003. We used the 80 cm IAC80 telescope (Teide Observatory) and the Tromsø-Texas photometer with an integration time of 10 s. Typical runs lasted for about 2.5–4 h on each target. Due to its brightness ($B = 11.8$), BA09 is a suitable object to be observed with this relatively small telescope. The data presented here for BA09 were obtained during the last night of observations under excellent photometric conditions; a large oscillation amplitude was already evident on the controller PC screen. We started observing BA09 at 23:43:10 UT on September 4, 2003 using the Quilt9 data acquisition software (Nather et al. 1990). The total length of the data set is 5h14m50s, but there were two interruptions of 7m20s and 39m40s respectively due to instrumental problems. The useful length of data, 4h27m50s, yields a resolution of $63 \mu\text{Hz}$. Figure 1 shows the total light curve of BA09, after sky subtraction and extinction correction,

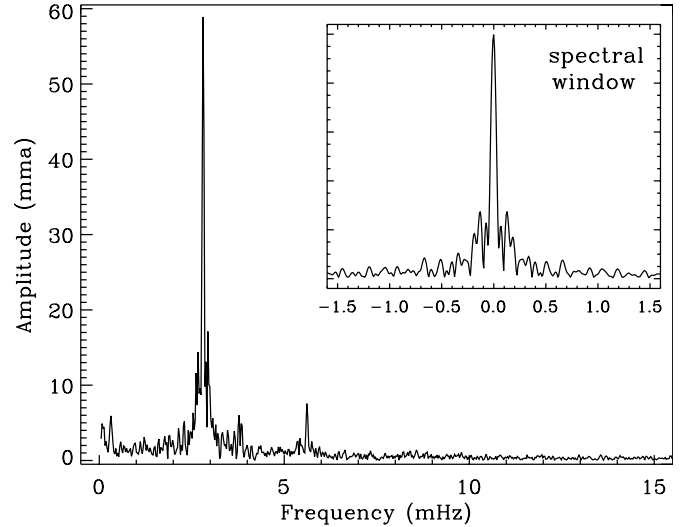


Fig. 2. Amplitude spectrum in units of milli-modulation amplitude (see text for details) obtained by fitting to sinusoidal functions the light curve in Fig. 1. The spectral window is shown in the insert.

Table 1. Frequency, period, amplitude and phase of the pulsations detected in the amplitude spectrum of BA09. Phases start at 23:43:10 UT on Sep. 4, 2003.

	Freq. (mHz)	Period (s)	Amplitude (mma)	Phase
ν_1	2.81	356	59.6	0.582
ν_2	5.62	178	8.2	-0.540
ν_3	3.78	264	5.6	1.139

with the gaps mentioned above. The data are represented by plus-symbols (+), while a synthetic light curve generated from the derived frequencies is plotted as a continuous line. The signal is expressed in units of milli-modulation intensity (mma)¹.

We used a standard sinusoidal fitting technique to obtain the amplitude spectrum showed in Fig. 2. In the upper-right area of this figure, we have plotted the spectral window, computed by fitting $\sin \omega_1 t$ to sinusoidal functions, ω_1 being the main frequency of BA09 ($\nu_1 = 2.81$ mHz) and t the vector of time with useful data. The spectral window's peak has a full width at half maximum of $64 \mu\text{Hz}$, that, as expected, coincides with the resolution given by the observational time interval. In the amplitude spectrum of the star a dominant peak of 59.6 milimodulation amplitude (1 mma \approx 1 mmag) can be seen. Within our resolution, it corresponds to a single oscillation frequency (ν_1). Two additional peaks with lower amplitudes (ν_2, ν_3) are also present. Table 1 gives the detected frequencies of the three peaks, with their associated amplitudes and phases.

In Fig. 3 we have used the prewhitening technique to calculate the residual spectrum after subtracting the main frequencies. At the top of Fig. 3 we show the complete amplitude spectrum of BA09. The second panel corresponds to the amplitude spectrum after subtracting the ν_1 frequency. In the third panel the amplitude spectrum after subtracting ν_1 and ν_2 is shown and

¹ Modulation intensity corresponds to the relative number of counts compared to the mean value. See Winget et al. (1994).

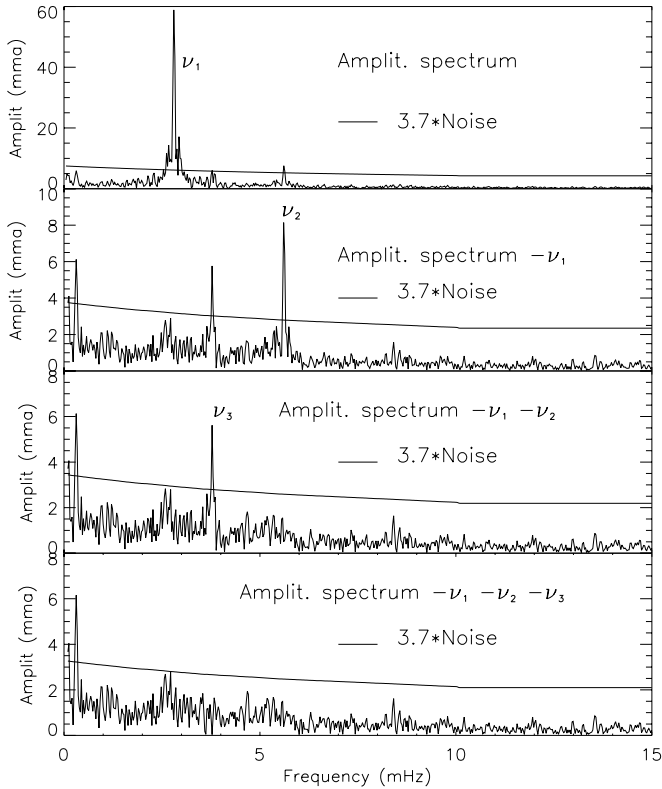


Fig. 3. Amplitude spectrum of BA09, before and after prewhitening of each of the three significant peaks (see text for details). The curved line corresponds to 3.7 times the noise level.

in the bottom panel ν_1 , ν_2 and ν_3 were eliminated. In all the panels we have indicated 3.7 times the noise level, calculated by averaging the amplitudes around each frequency in a wide frequency range. In this way, for the top panel, the level of the noise is overestimated, as we are including the large amplitude of the main peak in the calculations. In the last panel of Fig. 3 there is an additional peak above 3.7 times the noise level, at a frequency of about 0.3 mHz, but we do not consider this peak as definitive because it could be due to atmospheric fluctuations or instrument drift. A larger observational run is required to confirm it. Regarding the frequencies detected, we note that $\nu_2 = 2\nu_1$, strongly suggesting that the oscillation mode with frequency ν_1 is not a plain sinusoidal function, as found in other high amplitude EC14026 stars.

2.2. Spectroscopy

Following our discovery of pulsations in BA09, we obtained an intermediate resolution spectrum of that star using the ISIS spectrograph at the 4.2 m William Herschel Telescope on September 12th, 2003. The spectrum consists of a pair of 900 s integrations, one on the blue arm of the spectrograph through the R600B grating ($0.45 \text{ \AA}/\text{pix}$) centered at 4500 \AA , and a second on the red arm through the R158R grating ($1.63 \text{ \AA}/\text{pix}$) centered at 7500 \AA . Here we consider only the blue part of the spectrum. This spectrum allows us to fit the Balmer lines from $H\beta$ up to H_{13} , and the neutral He lines at 4472, 4026, 4922 and 5016 \AA . He II at 4686 \AA is included in the fit

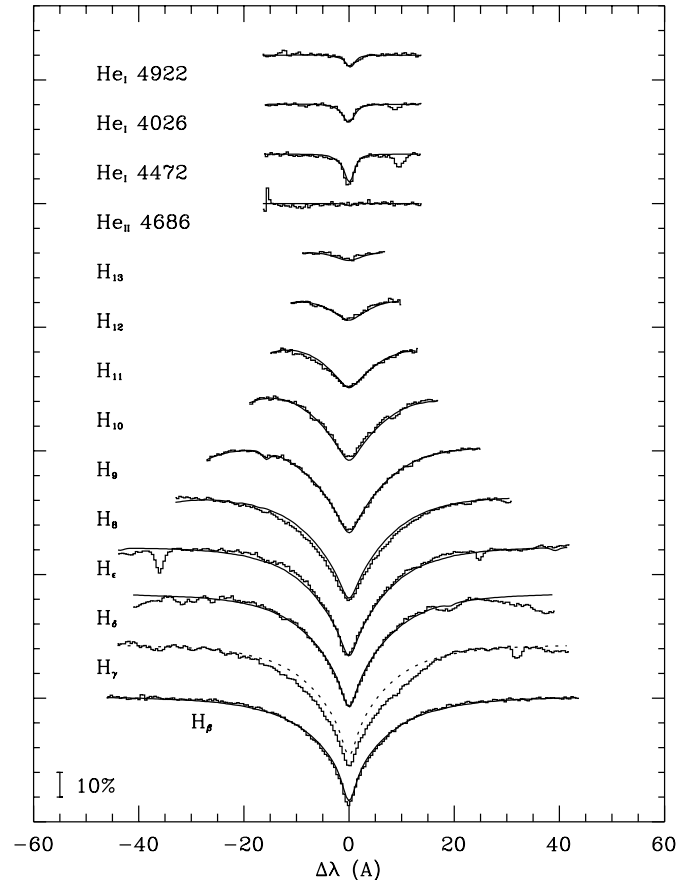


Fig. 4. LTE model fit to Balmer and Helium lines in the optical spectrum of Balloon 090100001.

although the line is not seen, in order to provide an additional fitting constraint. We have used the line blanketed LTE spectral synthesis model atmospheres of Heber et al. (2000), fitted with the χ^2 procedure of Bergeron et al. (1992) and updated to three dimensions by Saffer et al. (1994) in order to incorporate Helium abundance into the simultaneous fitting of effective temperature and gravity. The resulting best fit is shown in Fig. 4, and the parameters are listed in Table 2 followed by the formal fitting errors and a more realistic estimate of the systematic errors. Some lines, especially $H\gamma$, appears to fit poorly to the spectrum. This is entirely due to a series of ripples introduced into the spectrum by ISIS' dichroic that on occasions yields a poor calibration quality; a well known feature of this instrument when both arms are used simultaneously. For this reason $H\gamma$ has been completely kept out of the fit, as indicated by the dotted line in Fig. 4. The fit can still be considered as very good, due to the inclusion of the high order Balmer lines and He lines.

3. Discussion

Although within errors our new determinations of the physical parameters of BA09 agree with those of BBL91, the former are more accurate (see Table 2). The new values of T_{eff} and $\log g$ are marked with an asterisk in Fig. 5, putting BA09 in a quite different place in the EHB than BBL91's values do. Our new parameters move BA09 from the middle of the EC14026

Table 2. Physical parameters of BA09 obtained by BBL91 (with upper limit errors) and in this work. Our errors are formal fitting errors followed by a more realistic estimate of possible systematic errors.

	BBL91	This work
T_{eff} (K)	$32\,500 \pm 6700$	$29\,446 \pm 81 \pm 500$
$\log g$	6.00 ± 0.69	$5.33 \pm 0.02 \pm 0.10$
$\log n(\text{He})/n(\text{H})$	< -2.00	$-2.54 \pm 0.03 \pm 0.20$

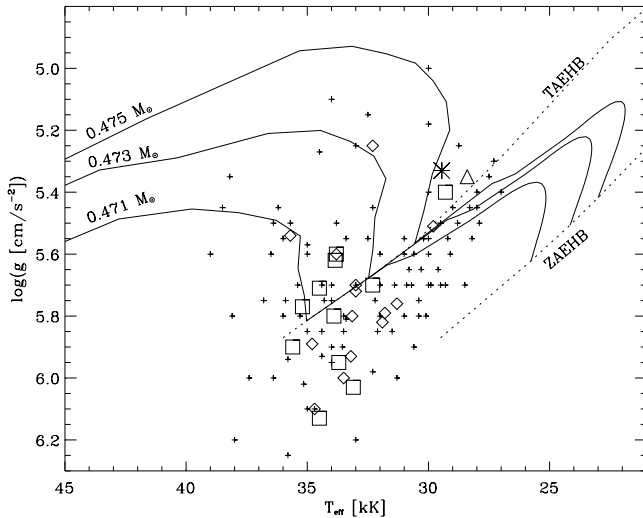


Fig. 5. Location of BA09 (marked with an asterisk) in the EHB area of the $(T_{\text{eff}}, \log g)$ plane, plotted together with constant sdBs (plus-symbols), pulsating sdBs (squares or diamonds) and 3 evolutionary tracks from Dorman et al. (1993). The diamond to the left of BA09 corresponds to PG 1605+072, while the square below is HS 2201+2610. The triangle to the right of the latter corresponds to HS 0702+6043 and the diamond below HS 2201+261 to Feige 48.

instability region to the cool and low gravity end. Other EC14026 stars are indicated in this figure (see figure caption), together with 3 evolutionary tracks of sdBs (from Dorman et al. 1993), as well as the Zero Age Extended Horizontal Branch (ZAEHB) and Terminal Age Extended Horizontal Branch (TAEHB). The new position of BA09 places it close to the cool group formed by HS 0702+6043, HS 2201+261 and Feige 48. Comparing the amplitude spectra of these stars, BA09 is similar to them in regard to the low number of periods of pulsation, but if we look at the amplitude of the main oscillation frequency it is more like PG 1605+072, as PG 1605+072 and BA09 have the greatest amplitudes of all the EC14026 stars known so far.

If we compare the evolutionary tracks showed in Fig. 5 with the location of BA09, it seems the star is a post core He-burning object as it is on the left of the TAEHB. If true, BA09 would be evolving very quickly away from the sdB area. In that case, BA09 would be an interesting object for studying changes in pulsating properties as it evolves, as proposed for HS 2201+2610 by Silvotti et al. (2002). Another possibility is that BA09 would still be in the He-core burning phase since we cannot reject that different models than those considered in

Fig. 5 (Han et al. 2002; Oreiro et al. 2003), or that systematic errors in the determination of T_{eff} and $\log g$ could place BA09 at the end of the He-core burning phase.

The frequency changes of, at least, the p modes are dominated by the dynamical time scale: $t_{\text{dyn}} = (G\bar{\rho})^{-1/2}$, where $\bar{\rho}$ is the mean density. Then a decrease in $\bar{\rho}$ (as it happens during most of the core-He burning phase of an sdB) means an increase in t_{dyn} and hence a decrease in the frequencies. In particular, we have calculated the variation with time of an $\ell = 0, n = 1$ mode (the fundamental radial one) of an $0.47 M_{\odot}$ sdB model. During the core He burning phase where $\bar{\rho}$ decreases, the change in the frequency is at most $dv/dt = -2 \times 10^{-11}$ Hz/yr. Similar results were obtained with different models (for details on the models see Oreiro et al. 2003; see also Charpinet et al. 2002b, whose results are very similar). During the last phase of He-core burning, where $\bar{\rho}$ increases, we find a frequency change of the order of $+10^{-10}$ Hz/yr. After core He exhaustion a faster evolution, and hence a larger change in the frequencies, is expected. This is confirmed by the fact that, for the same mode, after core-He exhaustion, we obtain a frequency change up to $dv/dt = -1.6 \times 10^{-6}$ Hz/yr. It is possible to achieve the required precision for a measurement of the rate of frequency change in the near future, hence providing the evolutionary stage of BA09.

The break-up rotational frequency of the star is about 0.26 mHz (assuming rigid rotation). Thus the main observed peak cannot be directly related to rotation. When comparing the frequencies of sdB models, with suitable values of T_{eff} and $\log g$, with the frequencies in Table 1 we find that the latter can correspond to either low order p modes of an evolved sdB star or low order g-modes of a younger one.

It is interesting to consider the frequency ratio $\nu_1/\nu_3 = 0.74$ (as commented earlier ν_2 seems to be just a harmonic of ν_1). Frequency ratios of p modes are in general much less sensitive to the details of stellar structure than frequencies. When comparing the observed ratio given above with the theoretical ones of a model near the core-He exhaustion we find that

$$\frac{\nu(\ell = 0, n = 1)}{\nu(\ell = 0, n = 2)} = 0.74 \quad \frac{\nu(\ell = 1, n = 1)}{\nu(\ell = 1, n = 2)} = 0.73$$

which suggest that ν_1 and ν_3 are two p modes with consecutive radial order. The same value of ℓ is not necessary, as the ratio between $\nu(\ell = 2, n = 1)$ (first overtone) and $\nu(\ell = 0, n = 1)$ (fundamental) is 0.72, also close to the observed one.

Acknowledgements. Part of this work was supported by Ministerio de Ciencia y Tecnología under projects AYA2000-1691 and AYA2001-1371. R. Oreiro acknowledges CajaCanarias for its financial support. We thank the Centro de Supercomputación de Galicia for the use made of their computational facilities. We thank Prof. Uli Heber for the spectral model grids. We thank the referee for his/her detailed comments. Prof. Solheim and J. M. González Pérez are also thanked for their aid in the obtaining of the photometric observations of this work.

References

- Bergeron, P., Saffer, R. A., & Liebert, J. 1992, ApJ, 394, 228
 Bixler, J. V., Bowyer, S., & Laget, M. 1991, A&A, 250, 370

- Charpinet, S., Fontaine, G., Brassard, P., et al. 1997, *ApJ*, 483, L123
- Charpinet, S., Fontaine, G., Brassard, P., & Dorman, B. 2002a, *ApJS*, 139, 487
- Charpinet, S., Fontaine, G., Brassard, P., & Dorman, B. 2002b, *ApJS*, 140, 469
- Dorman, B., O'Connell, R. W., & Rood, R. T. 1993, *ApJ*, 419, 596
- Han, Z., Podsiadlowski, Ph., Maxted, P., Marsh, T., & Ivanova, N. 2002, *MNRAS*, 336, 449
- Heber, U. 1986, *A&A*, 155, 33
- Heber, U., Reid, I. N., & Werner, K. 2000, *A&A*, 363, 198
- Kilkenny, D., Koen, C., O'Donoghue, D., & Stobie, R. S. 1997, *MNRAS*, 285, 640
- Koen, C., O'Donoghue, D., Kilkenny, D., et al. 1998, *MNRAS*, 296, 317
- Nather, R., Winget, D. E., Clemens, J. C., Hansen, C. J., & Hine, B. P. 1990, *ApJ*, 361, 309
- Oreiro, R., Ulla, A., Pérez Hernández, F., et al. 2003, *Ap&SS*, in press
- Saffer, R., Bergeron, P., Koester, D., & Liebert, J. 1994, *ApJ*, 432, 351
- Silvotti, R., Janulis, R., Schuh, S. L., et al. 2002, *A&A*, 389, 180
- Winget, D. E., Nather, R. E., Clemens, J. C., et al. 1994, *ApJ*, 430, 839